Title
Seismic Demands in Column Base Connections of Steel Moment Frames

Journal
Earthquake Spectra, 34(3)

ISSN
8755-2930

Authors
Torres-Rodas, Pablo
Zareian, Farzin
Kanvinde, Amit

Publication Date
2018-08-01

DOI
10.1193/062317eqs127m

Peer reviewed

Seismic Demands in Column Base Connections of Steel Moment Frames

Pablo Torres-Rodas,[a)] M.EERI, Farzin Zareian,[a)] M.EERI, and Amit Kanvinde[b)]

Methods for the seismic design of base connections in steel moment frames are well-developed and routinely utilized by practicing engineers. However, design loads for these connections are not verified by rigorous analysis. This knowledge gap is addressed through nonlinear time history simulations using design-level seismic excitation that interrogate demands in column base connections in 2-, 4-, 8-, and 12-story steel moment frames, featuring base connections that reflect current U.S. practice. The results indicate that: (1) for exposed base plate connections, lower bound (rather than peak) estimates of axial compression are suitable for design because higher axial forces increase connection strength by delaying base plate uplift; (2) even when designed as pinned (as in low-rise frames), base connections carry significant moment, which can be estimated only through accurate representation of base flexibility; and (3) the failure of embedded base connections is controlled by moment, which may be estimated either through overstrength or capacity-based calculations. [DOI: 10.1193/062317EQS127M]

INTRODUCTION

Column base connections in steel moment frames resist combinations of axial force, moment, and shear force under a variety of loadings. Depending on the type of structure (e.g., low- versus mid- or high-rise) and the magnitude of forces that must be resisted, these connections are constructed as exposed base plate connections with anchor rods (for low-rise frames) or as embedded-type connections (for mid- to high-rise frames); see Figure 1a and 1b. The vast majority of research on column bases has focused on their response at a component level. This includes experimental and analytical investigations to develop a basic understanding of force transfer mechanisms in these connections (e.g., Astaneh et al. 1992 and Gomez et al. 2010 for exposed base plate type connections and Barnwell 2015 and Grilli and Kanvinde 2017 for embedded-type connections).

These studies have been synthesized into design documents for base connections, including the American Institute of Steel Construction's (AISC) *Design Guide One* (Fisher and Kloiber 2006) and the AISC *Seismic Design Manual* (2006), as well as the Structural Engineers Association of California *Structural/Seismic Design Manual Volume 1* (SEAOC 2015). More recent studies have addressed rotational flexibility of these connections (Kanvinde et al. 2012,

[a)] Department of Civil and Environmental Engineering, University of California, Irvine, Irvine, CA 92697; Email: zareian@uci.edu (FZ, corr. author)
[b)] Department of Civil and Environmental Engineering, University of California, Davis, Davis, CA 95616

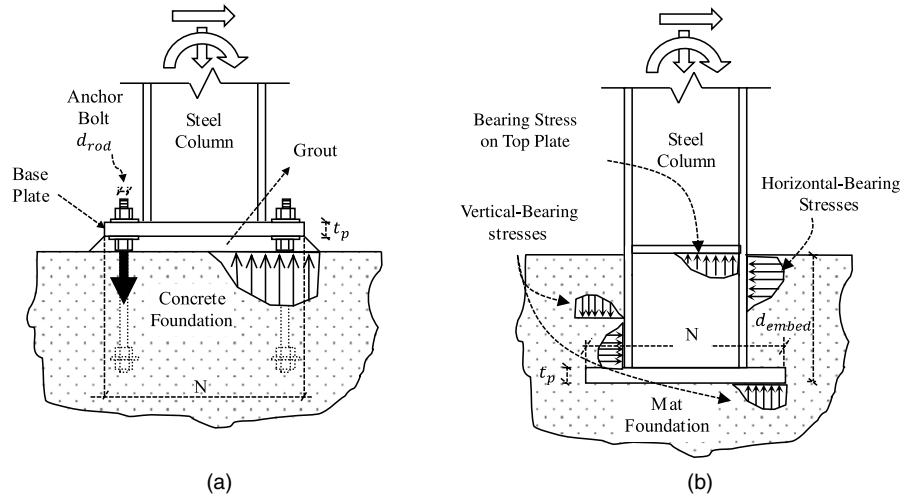

Figure 1. (a) Exposed base plate connection typical of low-rise construction and (b) embedded base plate connection typical of mid- to high-rise construction.

Torres-Rodas et al. 2017) and the effect of this flexibility on frame response (Zareian and Kanvinde 2013). Other work has focused on developing strategies for finite element simulation of column base connections (Kanvinde et al. 2013, Stamatopoulos and Ermopoulos 2011). The profusion of research in this area points to the importance of these connections. However, a closer examination of this research reveals that it has focused almost exclusively on connection response (including strength, stiffness, or hysteretic characteristics) and not on the axial force, moment, and shear demands for which these connections must be designed. Consequently, the connections are designed for force demands that notionally correspond to idealized modes of response, while these demands themselves are unsubstantiated by rigorous simulation. Specifically, both the SEAOC (2015) and AISC (2016) Seismic Design Manuals illustrate a "capacity-based" design of the base connections, such that it is designed for the moment $1.1R_yM_p$ of the connected column (consistent with a strain-hardened plastic hinge), accompanied by an axial force corresponding to the overstrength seismic load case (i.e., the $\Omega_0 E$ case), as determined from equivalent lateral load—or response spectrum—analysis. The intent of these guidelines is to ensure that the base connection itself remains elastic, inducing a plastic hinge in the column cross-section at the base. Contrary to this assumed behavior, numerous studies (e.g., Gupta and Krawinkler 1999, National Earthquake Hazards Reduction Program [NEHRP] 2010) indicate that for design-level ground motions, the first-story column may not develop a plastic hinge because a plastic mechanism is not formed or because a partial mechanism is formed (engaging only a few stories through the height of the structure). The choice of $\Omega_0 E$ for the axial force is similarly not supported by research; in fact, studies by Richards (2009) suggest that this may significantly overestimate axial forces in columns during design-level shaking.

Accurate characterization of demands in the base connection is critical because: (1) the geometric complexity and their location at the interface of two materials implies that

conservatisms in demand estimation entail significant expense (Gomez et al. 2010), or, conversely, (2) nonconservatism in demand estimation has the potential to compromise connections that transfer forces from the entire building into the foundation. Motivated by this, the main objective of this study is to characterize force and moment demands in column base connection to inform their design. The primary scientific basis for this study is a series of nonlinear response history analysis (NLRHA) simulations on steel special moment-resisting frames (SMRFs) representative of current U.S. construction using ground motions representing design-level seismic excitation. These simulations (which subject 2-, 4-, 8-, and 12-story frames to a suite of 40 design-level ground motions) reflect key aspects of structural response, including geometric and material nonlinearity and, perhaps more importantly, the rotational flexibility of the column base itself. The paper begins by reviewing current practice for designing column bases against the backdrop of research in the area. This is followed by a discussion of the design characteristics of the frames used in this study and the methodology used to simulate them. Design implications of the simulation results are then discussed before outlining limitations of the study.

BACKGROUND

Seismic design considerations for column bases are currently prescribed in the American National Standards Institute/American Institute of Steel Construction *ANSI/AISC 341-16 Seismic Provisions for Structural Steel Buildings* (2016), referred to hereafter as the *ANSI/AISC 341-16 Seismic Provisions* (2016). As per the *ANSI/AISC 341-16 Seismic Provisions* (2016), the bases must be designed for axial loads, shear forces, and moments that are the summation of the required connection strengths (in the vertical, horizontal, and rotational directions) for all the members attached to the column base. For SMRFs where the only element attached to the base is the column, this implies that the design axial force corresponds to the required axial strength of the column. In seismically active regions, this usually corresponds to the $1.2D^* + 0.5L + \Omega_0 E$ load case, in which D^* corresponds to the Dead Load, including the effects of vertical acceleration (American Society of Civil Engineers/Structural Engineering Institute *ASCE/SEI 7-10* 2006), L is the Live Load, and $\Omega_0 E$ is the "overstrength" seismic load. For special moment frames, $\Omega_0 = 3.0$ (*ANSI/AISC 341-16* 2016). Similar considerations apply to connection shear forces. For the flexural strength, the *ANSI/AISC 341-16 Seismic Provisions* (2016) require that either: (1) the base connection be designed for the fully yielded and strain hardened capacity (i.e., $1.1R_yM_p$ of the attached column) or (2) the connection be designed for the moment calculated using the overstrength seismic load (i.e., using the Ω_0- factor), provided that the connection or the foundation is able to accommodate inelastic rotation. As a practical matter, achieving the latter condition is challenging. This is because unlike for beam–column connections (for which prequalified connection details have been developed based on extensive testing, see *AISC 358-16* 2016), minimal guidance is available for design or detailing of base connections for ductile performance, implying that qualification tests must be conducted for this purpose. Consequently, designers usually select the former option (i.e., designing the base connection to remain elastic as the column reaches flexural capacity). This can be costly, especially in situations where large design forces (essentially corresponding to yielding of the column flanges) must be transmitted into concrete, usually through anchors or other attachments, subject to the requirements of the American Concrete Institute *ACI 318-14* (2014,

Appendix D). In addition to the practical challenges of achieving ductile performance, the requirement that the base be designed for overstrength seismic loads is somewhat arbitrary, even if motivated by caution. Specifically, it contrasts with design criteria for other elements in the structure (e.g., beams, in which inelastic action is expected), which are designed for the reduced seismic load without the Ω_0- factor. Second, it does not define ductile performance (e.g., connection rotation capacity) that qualifies for overstrength-based design. Owing to these issues, design manuals from both the SEAOC (2015) and AISC (2006) illustrate the use of the former condition (i.e., designing the base connection for the column moment $1.1R_yM_p$) and an axial load corresponding to the overstrength seismic load.

As discussed earlier, NLRHA simulations (Richards 2009) have shown that capacity-based design approaches, as well as overstrength seismic loads, may significantly overestimate demands in columns. For column bases, demands may be incorrectly estimated for the following reasons: (1) in high-rise frames, response is often dominated by higher modes resulting in the formation of partial-story mechanisms, such that plastic hinges may not form at the base of the column, suggesting that capacity design using $1.1R_yM_p$ is conservative; (2) for all frames (particularly low-rise frames) column bases have significant rotational flexibility with respect to the fixed-based assumption typically used for calculation of design loads. Although this flexibility is detrimental to overall structural performance, it has the effect of reducing flexural demands at the base of the column (Zareian and Kanvinde 2013); and (3) the peak axial forces and moments may not occur synchronously.

In summary, current guidelines for the seismic design of column bases are not rigorously informed by nonlinear time history simulation, and are formulated conservatively based on assumptions of idealized frame response and intuitive reasoning. Although well-intentioned, these bear closer scrutiny, given the critical function of these connections (transferring forces from the entire building) and the high cost of overestimating design forces. Against this backdrop, the specific objectives of the study are: (1) to develop fundamental understanding of axial force, moment, and shear demands in column base connections in a range of (2-, 4-, 8-, and 12-story) steel moment frames under design-level ground motions; and (2) based on this understanding, to recommend optimal approaches for the design of these connections. The next section summarizes the archetype frames considered in this study.

ARCHETYPE STEEL MOMENT FRAMES AND BASE CONNECTIONS

As discussed in the previous section, four steel moment frames were considered in this study. The overall geometry of these frames and member sizes are shown in Figure 2. This study takes the approach of using "archetype" frames to develop fundamental and broad insights about system behavior, focusing on one variable (i.e., building height or number of stories), which is anticipated to have the most significant impact on the seismic demands in the base connections. Referring to Figure 2, the frames range in height from 8.5 m (2-story) to 48.2 m (12-story), each with three bays, and are designed as the seismic load resisting system for buildings with an identical floor plan, which is also shown in Figure 2.

The buildings are designed as per *ASCE/SEI 7-05* (2006), and the *ANSI/AISC 341-10 Seismic Provisions* (2010), assuming $R = 8$, and site class D conditions under the seismic design category $D_{\max}$. Seismic hazard and site conditions consistent with a non-near fault location in the Los Angeles basin are assumed. The fundamental time periods of the

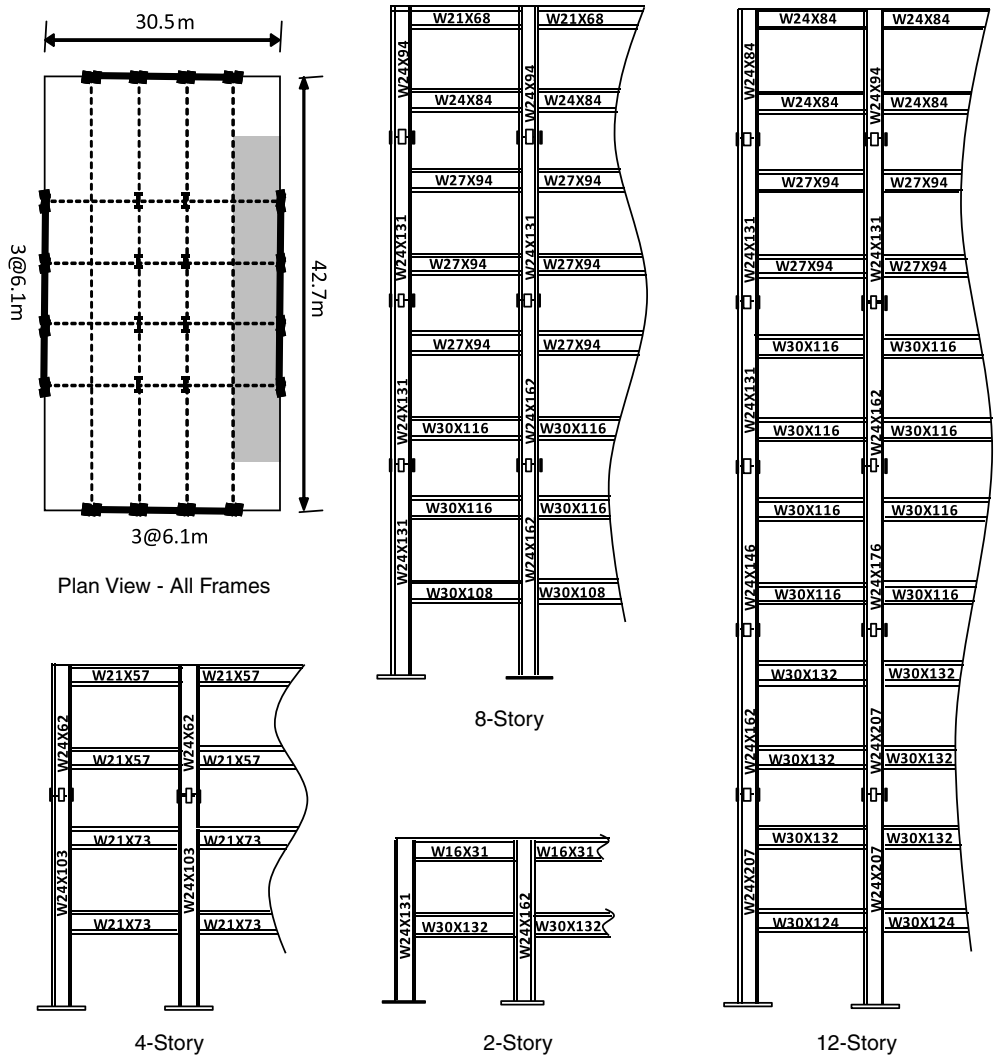

Figure 2. Key characteristics of the moment-resisting frames used in this study.

2-, 4-, 8-, and 12-story frames are 0.95, 1.65, 2.33, and 3.36 s, respectively—these are superimposed on the design spectrum, as shown in Figure 3. Other characteristics of these buildings are detailed in Zareian and Kanvinde (2013). For the purposes of this study, these buildings represent archetype SMRFs designed as per code, in which the demands on base connections may be examined.

As discussed previously, rotational flexibility of the base connections themselves has significant impact on the force and moment demands in the base connections. However, the flexibility of the base connections depends on their design (i.e., configuration, sizing of various elements), which, in turn, depends on the loads for which they are designed.

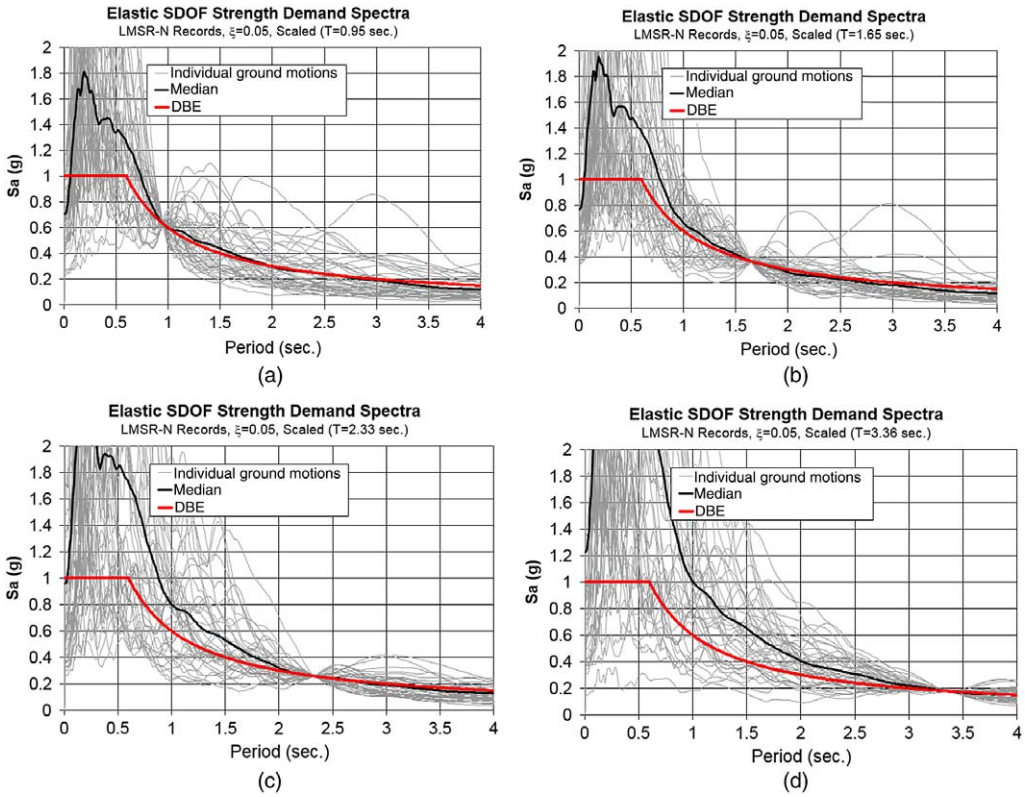

Figure 3. Response spectra scaled to the first period of the SMRFs: (a) 2-story, (b) 4-story, (c) 8-story, and (d) 12-story.

To resolve this circularity, the following process was adopted for design of the connections and subsequent assessment:

1. For each frame, linear elastic analyses were conducted under code specified (*ASCE/SEI 7-05* 2006) Dead, Live, and Earthquake loads. For the earthquake load case, the total base shear for each frame was determined using the design spectrum shown in Figure 3 and an equivalent lateral load distribution that distributes the base shear in an exponential manner (depending on the code specified period) through the height of the building, as per *ASCE/SEI 7-05* (2006). This results in the basic load cases for Dead, Live, and Earthquake loads, which may be factored as necessary within various load combinations. For the 2-story frame, the bases are simulated as pinned in these linear analyses. In all the other frames, the base connections are simulated as fixed. This reflects prevalent U.S. practice as base connections are often designed (and simulated) as pinned in low-rise frames and fixed in mid- to high-rise frames.
2. For each of the two (interior and exterior) base connections within each frame, a range of possible design load combinations were considered for design. These are based on the linear elastic analyses described in the previous point, as well as on the capacity of adjoining elements. Specifics of the simulations are as follows:

- For the 2-story frame, two combinations were considered; these correspond to two levels of axial load (i.e., $P = 1.2D^* + 0.5L + \Omega_0 E$, and $P = 1.2D^* + 0.5L + Q$, where Q represents the summation of shears in all beams framing into the column, assuming all the beams are yielded and strain hardened). Since the bases were assumed pinned, the base moment in both these cases is zero.
- For the 4-story frame, four load combinations were considered. These correspond to two estimates of axial force: $P = 1.2D^* + 0.5L + \Omega_0 E$ and $P = 1.2D^* + 0.5L + Q$ and two estimates of bending moment (i.e., $M = 1.2D^* + 0.5L + \Omega_0 E$, and $M = 1.1R_y M_p$ of the connected column). Recall that unlike the 2-story frame, bases of the 4-story frame are simulated as fixed, resulting in the development of base moments.
- For the 8- and 12-story frames, four load combinations are considered. These arise from two estimates of base moment (i.e., $M = 1.2D^* + 0.5L + \Omega_0 E$, and $M = 1.1R_y M_p$ of the connected column) multiplied with two estimates of column shear, (i.e., $V = 1.2D^* + 0.5L + \Omega_0 E$, and $V = 2 \times 1.1R_y M_p / L_{column}$). Note that the combinations for the 2- and 4-story frames include variations in axial load, whereas those for the 8- and 12-story frames include variation in the shear, but not axial load. This distinction is based on current construction practice. Specifically, exposed base connections (Figure 1a) are common in low-rise frames (2- and 4-story frames in this study). Current design methods for exposed base plates (Fisher and Kloiber 2006, Grilli and Kanvinde 2013) reflect interactions between the axial force and moment, as both are resisted by anchor rod tension and are relatively insensitive to shear. On the other hand, embedded base connections (Figure 1b) are common mid- to high-rise frames (8- and 12-story frames in this study)—primarily because it is economically unfeasible to transfer large base moments through anchor rods. Design methods for these reflect interactions between shear and moment, as both are resisted by horizontal bearing stresses in the concrete and are relatively insensitive to axial force. Following this, the load combinations outlined previously result in realistic designs of base connections consistent with current practice. Also note that some possible load combinations (e.g., axial forces, moments, or shears corresponding to the reduced seismic load $M = 1.2D^* + 0.5L + 1.0E$) are omitted, as they are likely to be unconservative and cannot be rationalized for components that are not explicitly detailed for ductility.

3. For all the frames, sets of base connections (consisting of interior and exterior column connections) are designed to satisfy each of the load combinations discussed previously. As discussed previously, the exposed base plate connections are designed for the 2- and 4-story frames, whereas embedded base connections are designed for the 8- and 12-story frames. Design of the exposed base plate connections is carried out as per the process outlined in *Steel Design Guide One* (AISC 2006) and Gomez et al. (2010). Design of the embedded base connections is carried out as per an approach recently proposed by Grilli and Kanvinde (2017). Table 1 details the dimensions and configurational aspects of each set of base connections

designed in this way. For all designs, a nominal concrete strength $f'_c = 27.6$ MPa was assumed.

4. The previous process results in a multiple base connection sets for each of the frames, corresponding to the 14 load combinations (two for the 2-story frame and four for each one of the taller frames) outlined previously in point 2. The first two columns of Table 1 list the loadings for which the various combinations were designed, whereas the remaining summarize the key parameters of each base connection. Each of these configurations (i.e., frame and base connection combination) was subsequently simulated through NLRHA, with the appropriate base

Table 1. Design configurations

2-Story frame

		Interior column base					Exterior column base				
P^{base}_{design}	M^{base}_{design}	B[a]	N	t_p	d_{rod}[b]	β[c] ($\times 10^4$)	B	N	t_p	d_{rod}	β ($\times 10^4$)
$1.2D + 0.5L + \Omega_0 E$	N/A	508	762	25	25	1.16	508	762	25	25	1.16
$1.2D + 0.5L + Q$	N/A	508	762	25	25	1.16	508	762	25	25	1.16

4-Story frame

		Interior column base					Exterior column base				
P^{base}_{design}	M^{base}_{design}	B	N	t_p	d_{rod}	β ($\times 10^5$)	B	N	t_p	d_{rod}	β ($\times 10^5$)
$1.2D + 0.5L + \Omega_0 E$	$1.2D + 0.5L + \Omega_0 E$	508	762	57	44	2.84	508	762	51	38	2.47
$1.2D + 0.5L + \Omega_0 E$	$1.1R_yM_p$	508	762	51	44	2.80	508	762	44	38	2.49
$1.2D + 0.5L + Q$	$1.2D + 0.5L + \Omega_0 E$	508	762	51	44	2.96	508	762	51	38	2.47
$1.2D + 0.5L + Q$	$1.1R_yM_p$	508	762	44	38	2.66	508	762	44	38	2.49

8-Story frame

		Interior column base					Exterior column base				
V^{base}_{design}	M^{base}_{design}	d_{emb}[d]	b_f	B	N	β ($\times 10^5$)	d_{embed}	b_f	B	N	β ($\times 10^5$)
$1.2D + 0.5L + \Omega_0 E$	$1.2D + 0.5L + \Omega_0 E$	864	508	762	762	2.87	660	328	762	762	2.10
$1.2D + 0.5L + \Omega_0 E$	$1.1R_yM_p$	1016	711	914	914	3.32	1067	508	914	914	2.82
$2 \times 1.1R_yM_p/L_{column}$	$1.2D + 0.5L + \Omega_0 E$	914	508	762	762	2.89	762	328	762	762	2.18
$2 \times 1.1R_yM_p/L_{column}$	$1.1R_yM_p$	1016	711	914	914	3.26	1067	508	914	914	2.76

12-Story frame

		Interior column base					Exterior column base				
V^{base}_{design}	M^{base}_{design}	d_{embed}	b_f	B	N	β ($\times 10^5$)	d_{embed}	b_f	B	N	β ($\times 10^5$)
$1.2D + 0.5L + \Omega_0 E$	$1.2D + 0.5L + \Omega_0 E$	965	711	864	864	3.73	864	610	762	762	3.58
$1.2D + 0.5L + \Omega_0 E$	$1.1R_yM_p$	1016	965	1016	1016	3.88	1016	965	1016	1016	3.92
$2 \times 1.1R_yM_p/L_{column}$	$1.2D + 0.5L + \Omega_0 E$	965	711	864	864	3.64	864	610	762	762	3.41
$2 \times 1.1R_yM_p/L_{column}$	$1.1R_yM_p$	1016	965	1016	1016	3.81	1016	965	1016	1016	3.81

[a] B, N, and t_p are base plate dimensions in mm; see Figure 1a and 1b (B is the width of the base plate and an out-of-plane dimension that is not shown in Figure 1a and 1b.
[b] d_{rod} is anchor rod diameter, with two anchor rods in each line; see Figure 1a.
[c] β is the estimated rotational stiffness of the designed base (kN · m/rad).
[d] d_{emb} is embedment depth and b_f is width of embedded portion; see Figure 1b.

flexibility (as discussed in the next section) to characterize the axial force and moment demands in the base connections.

NLRHA (discussed in the next section) on these 14 configurations provides the best estimates of base forces and moments, appropriately considering the effects of base flexibility for each configuration. As a result, these forces and moments may be compared with base connection capacities to determine which load combinations result in successful (safe and nonconservative design). When conducted in this way, these comparisons are consistent in terms of the interactive relationships between base flexibility, the force/moment demands, and the base strength capacities.

SIMULATION METHODOLOGY AND MODELS

Each of the 14 combinations discussed previously were simulated using the platform OpenSEES (McKenna et al. 2000). Referring to Figure 4, all configurations were simulated as two-dimensional (2-D) planar frames. The main aspects of these models are summarized later:

1. The beams and columns were simulated as elastic elements with concentrated plasticity (i.e., rotational $M - \theta$ hinges) at their ends. The inelastic response of these hinges was represented through a hysteretic model (i.e., bilinear) developed by Ibarra et al. (2005), which consists of a bilinear rise, linear "cap" monotonic backbone supplemented by rules (developed by Lignos and Krawinkler 2011 and Zareian and Krawinkler 2009) to model the energy-based cyclic deterioration of strength and stiffness, as well as the onset of the cap (i.e., loss of deformation capacity). The parameters for the backbone and the hysteresis are calibrated from a compilation of 300 component tests assembled by Lignos and Krawinkler (2011).

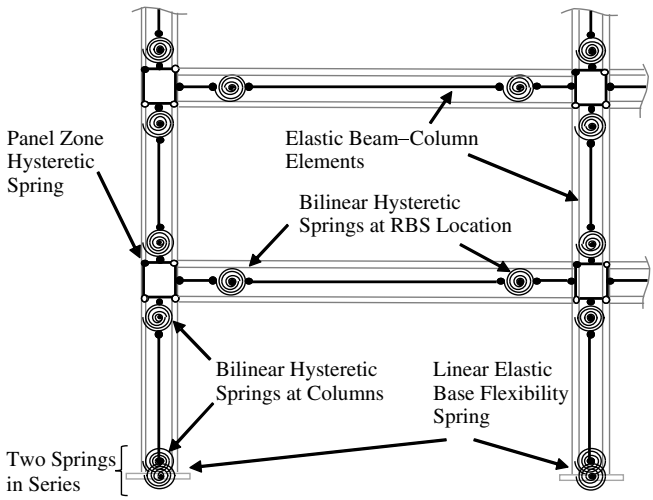

Figure 4. Schematic representation of the physical and mathematical model for moment-resisting frames.

These springs cannot directly simulate axial force–moment interactions in the columns. To address this, the moment strength of the hysteretic backbone is modified using suitable interaction equations (AISC 2011) and axial loads obtained from combined actions of gravity and lateral loading (estimated as $P_{1.2D*+0.5L} + 0.5 \times P_{\Omega_0 E}$, in which the latter term reflects the average lateral load because of cyclic earthquake motions).

2. Panel zone effects (i.e., finite size as well as deformations) were modeled through a parallelogram element with a nonlinear hysteretic hinge (see Figure 4), whose strength and stiffness properties are determined as per the Applied Technology Center *ATC 72-1* (2010).
3. Destabilizing $P - \Delta$ effects were modeled through a "leaning-column," in conjunction with a large displacement formulation to simulate sidesway collapse. This leaning column was loaded with vertical loads corresponding to the lateral as well as the gravity system.
4. Column bases were simulated as elastic rotational springs (see Figure 4). Simulating these bases as elastic is consistent with current design practice (and intent of the *ANSI/AISC 341-16 Seismic Provisions* 2016) as discussed earlier. For all configurations that used exposed base connections (i.e., the 2- and 4-story frames), the rotational stiffness for each base connection was calculated using an approach proposed by Kanvinde et al. (2012), which was later validated by Trautner et al. (2016). For the configurations that used embedded base connections (i.e., the 8- and 12-story frames), the stiffness for each base connection was determined using an approach developed by Torres-Rodas et al. (2017). Both of these approaches determine the rotational stiffness of the base connections by aggregating deformations of various components (e.g., base plate, anchor rods, concrete, and the soil underlying the foundation) under applied forces. Table 1 (introduced previously) also summarizes the base connection stiffness determined in this manner for all connections; this is denoted as β. The true base connection stiffness may vary significantly with respect to the estimated value for three reasons. First, the models for estimating base connection stiffness are susceptible to error because they are calibrated only based on limited test data. The cited references (Kanvinde et al. 2012, Torres-Rodas et al. 2017) note that this error may be on the order of 10% to 20%. Second, multiple designs (e.g., combinations of plate thickness, anchor rod size, footing type) are often possible for the same design forces, based on local construction practice, soil bearing capacity, and cost of labor versus material. Third, construction tolerances, as well as variation between actual and specified values of material properties, have the potential for introducing additional error. Recognizing these sources of error, the sensitivity of the all results to base connection stiffness is rigorously examined. To this end, each of the configurations listed in Tables 1 is simulated with three sets of base flexibility: one reflects the best estimate of base flexibility (i.e., the rotational springs at the interior and external column use the values of β listed in Table 1). Two additional sets of simulations are conducted, with the rotational springs assigned the values $\beta/2$ and 2β to account for sufficiently large variation in the base stiffness with respect to the best estimate.

The previous process results in 42 simulation models, with three corresponding to each configuration shown in Table 1. Each of the models was subjected to a suite of 40 California ground motions selected by Medina and Krawinkler (2003), scaled to match the design-level shaking (i.e., corresponding to a probability of exceedance of 10% in 50 years, 10/50) at the first mode period of the structure for typical soil type D in the Los Angeles area. Figure 3 shows the scaled spectra, as well as the equal hazard spectrum (i.e., random component). For each building, the spectra are scaled to match the target spectrum at the fundamental period of each building.

For each simulation run, time histories of moments, axial forces, and shear forces (at all bases) were recorded. Determining design criteria from these time histories is not straightforward for two reasons. First, the base moment and the axial load do not peak at the same time in any of the time histories, owing to complex dynamic response; this means that using a combination of the peak axial forces and moments for design may not accurately reflect instantaneous demands. Second, connection capacity (especially for the exposed base plate connections) is controlled by interaction between axial force and moments (see Gomez et al. 2010). In such cases, neither the peak moment nor the axial force may control design; rather, a combination of intermediate values of both the moment and force may be critical owing to the shape of the capacity interaction curve. Another issue is the interpretation of variability in response between the various ground motions for the same configuration. As the 40 ground motions correspond to design-level shaking (i.e., 10/50 events), it is posited that an acceptable design criterion is one that results in safe design for all the ground motions. Considering these various factors, quantities of interest are derived from each time history and summarized in Table 2. These quantities are briefly introduced later; a detailed discussion interpreting these quantities in the context of design follows in a subsequent section:

1. The maximum (over all ground motions) of the peak values from each of the time histories of axial force, moment, and shear; these are denoted $P_{\max}$, $M_{\max}$, and $V_{\max}$. Each of these actions is normalized by the axial force, moment, or shear corresponding to (a) the overstrength seismic load (i.e., $1.2D^* + 0.5L + \Omega_0 E$) and (b) a capacity-based estimate corresponding to the particular action. For example, the peak axial force $P_{\max}$ is normalized by P_Q, which reflects the summation of beam shears in all, in addition to the axial load in the base corresponding to $1.2D^* + 0.5L$. The peak shear $V_{\max}$ is normalized by $2 \times 1.1R_yM_p/L_{column}$, consistent with reverse curvature bending of the column with plastic hinges at both ends. The peak moment $M_{\max}$ is normalized by $1.1R_yM_p$. Normalization in this way enables the assessment of these demands relative to commonly used design forces and member capacities. The quantities shown in Table 2 correspond only to the best estimate of base stiffness β, as summarized previously in Table 1.
2. An index α quantifies the margin of safety of the base connections given vector-valued demands (consisting of multiple force actions, i.e., P and M for the exposed connections and V and M for the embedded connections) and corresponding capacities, defined by interactions between these force actions. Figure 5a and 5c illustrate the determination of α for interior and exterior connections from the 4-story frame; Figure 5b and 5d show similar information for embedded connections

Table 2. Summary of analysis results

2-Story frame

		$\frac{M_{max}}{M_{\Omega_0}}$[a]		$\frac{M_{max}}{1.1R_yM_p}$		$\frac{P_{max}}{P_{\Omega_0}}$[a]		$\frac{P_{max}}{P_Q}$[b]		$P_{min}(P_{\Omega_0})$[d]		$P_{min}(P_Q)$[d]		α_{max}	
P^{base}_{design}	M^{base}_{design}	I[b]	E[a]	I	E	I	E	I	E	I	E	I	E	I	E
P_{Ω_0}	NA	NA	NA	0.20	0.24	0.43	0.84	0.43	0.72	307.6 (−1108.94)	0.00 (−570.17)	307.6 (−1085.76)	0.00 (−887.87)	0.81	1.08
P_Q	NA	NA	NA	0.20	0.25	0.43	0.84	0.43	0.72	320.05 (−1108.94)	0.00 (−570.17)	320.05 (−1085.76)	0.00 (−887.87)	0.80	1.07

4-Story frame

P^{base}_{design}	M^{base}_{design}	$\frac{M_{max}}{M_{\Omega_0}}$		$\frac{M_{max}}{1.1R_yM_p}$		$\frac{P_{max}}{P_{\Omega_0}}$		$\frac{P_{max}}{P_Q}$		$P_{min}(P_{\Omega_0})$		$P_{min}(P_Q)$		α_{max}	
P_{Ω_0}	M_{Ω_0}	0.94	0.94	0.99	0.99	1.17	1.35	0.42	1.02	1029.76 (834.04)	588.5 (−31.58)	1029.76 (−1335.8)	588.5 (−957.7)	0.85	0.96
P_{Ω_0}	$1.1R_yM_p$	0.94	0.94	0.99	0.99	1.17	1.02	0.41	0.77	786.9 (834.04)	588.5 (−31.58)	786.9 (−1335.8)	588.5 (−957.7)	0.97	1.10
P_Q	M_{Ω_0}	0.95	0.94	0.99	0.99	1.17	1.02	0.41	0.77	786.9 (834.04)	588.5 (−31.58)	176.9 (−1335.8)	588.5 (−957.7)	0.97	0.96
P_Q	$1.1R_yM_p$	0.95	0.94	0.99	0.99	1.17	1.02	0.41	0.76	850.9 (834.04)	588.5 (−31.58)	191.3 (−1335.8)	588.5 (−957.7)	1.18	1.10

8-Story frame

V^{base}_{design}	M^{base}_{design}	$\frac{M_{max}}{M_{\Omega_0}}$		$\frac{M_{max}}{1.1R_yM_p}$		$\frac{P_{max}}{P_{\Omega_0}}$		$\frac{P_{max}}{P_Q}$		$\frac{V_{max}}{V_{\Omega_0}}$[a]		$\frac{V_{max}}{V_{M_p}}$[c]		α_{max}	
V_{Ω_0}	M_{Ω_0}	1.23	0.91	0.99	0.65	0.36	1.08	0.32	0.81	1.54	1.48	1.02	0.77	1.22	0.90
V_{Ω_0}	$1.1R_yM_p$	1.23	0.91	0.99	0.65	0.36	1.08	0.32	0.81	1.54	1.55	1.02	0.82	0.98	0.67
V_{Mp}	M_{Ω_0}	1.23	0.91	0.99	0.65	0.36	1.08	0.32	0.81	1.54	1.63	1.01	0.85	1.23	0.88
V_{Mp}	$1.1R_yM_p$	1.23	0.91	0.99	0.65	0.36	1.08	0.32	0.81	1.55	1.56	1.01	0.82	0.99	0.68

12-Story frame

V^{base}_{design}	M^{base}_{design}	$\frac{M_{max}}{M_{\Omega_0}}$		$\frac{M_{max}}{1.1R_yM_p}$		$\frac{P_{max}}{P_{\Omega_0}}$		$\frac{P_{max}}{P_Q}$		$\frac{V_{max}}{V_{\Omega_0}}$		$\frac{V_{max}}{V_{M_p}}$		α_{max}	
V_{Ω_0}	M_{Ω_0}	1.15	0.86	0.97	0.64	0.43	1.54	0.34	0.80	1.41	1.19	0.94	0.61	1.07	0.82
V_{Ω_0}	$1.1R_yM_p$	1.15	0.86	0.97	0.64	0.43	1.54	0.34	0.80	1.41	1.21	0.94	0.63	0.89	0.60
V_{Ω_0}	M_{Ω_0}	1.15	0.86	0.97	0.64	0.43	1.54	0.34	0.80	1.40	1.19	0.94	0.61	1.09	0.85
V_{Mp}	$1.1R_yM_p$	1.15	0.86	0.97	0.64	0.43	1.54	0.34	0.80	1.40	1.21	0.94	0.63	0.91	0.61

[a] $M_{\Omega_0}, P_{\Omega_0}, V_{\Omega_0} = 1.2D^* + 0.5L + \Omega_0 E$.
[b] $P_Q = 1.2D^* + 0.5L + \sum 2 \times 1.1R_yM_p^{beam}$.
[c] $V_{Mp} = 2 \times 1.1R_yM_p/L_{column}$.
[d] P_{min} is normalized by $P_{\Omega_0} = 1.2D^* + 0.5L - \Omega_0 E$, and $P_Q = 1.2D^* + 0.5L - \sum 2 \times 1.1R_yM_p^{beam}$.

from the 8- and 12-story frames. Specifically, these figures contain "particle plots" showing the coevolution of the demands, superimposed on the limit-state line (or interaction curve) between the axial force and moment for the exposed connection (Figure 5a) or the shear and moment for the embedded connection (Figure 5b). These curves are determined from the strength characterization approaches discussed earlier.

Referring to these figures, α is determined as a scale factor that, when applied equally to the vertical and horizontal coordinates of the interaction curve, results in exactly one point of the particle plot lying on the scaled interaction curve. When defined in this manner, α may be interpreted as a scalar demand-capacity ratio such that $\alpha > 1$ implies an unsafe condition whereas $\alpha \leq 1$ represents a safe condition. Table 2 lists the maximum value of $\alpha_{\max}$, reflecting the highest demand-capacity ratio attained over all 40 ground motions.

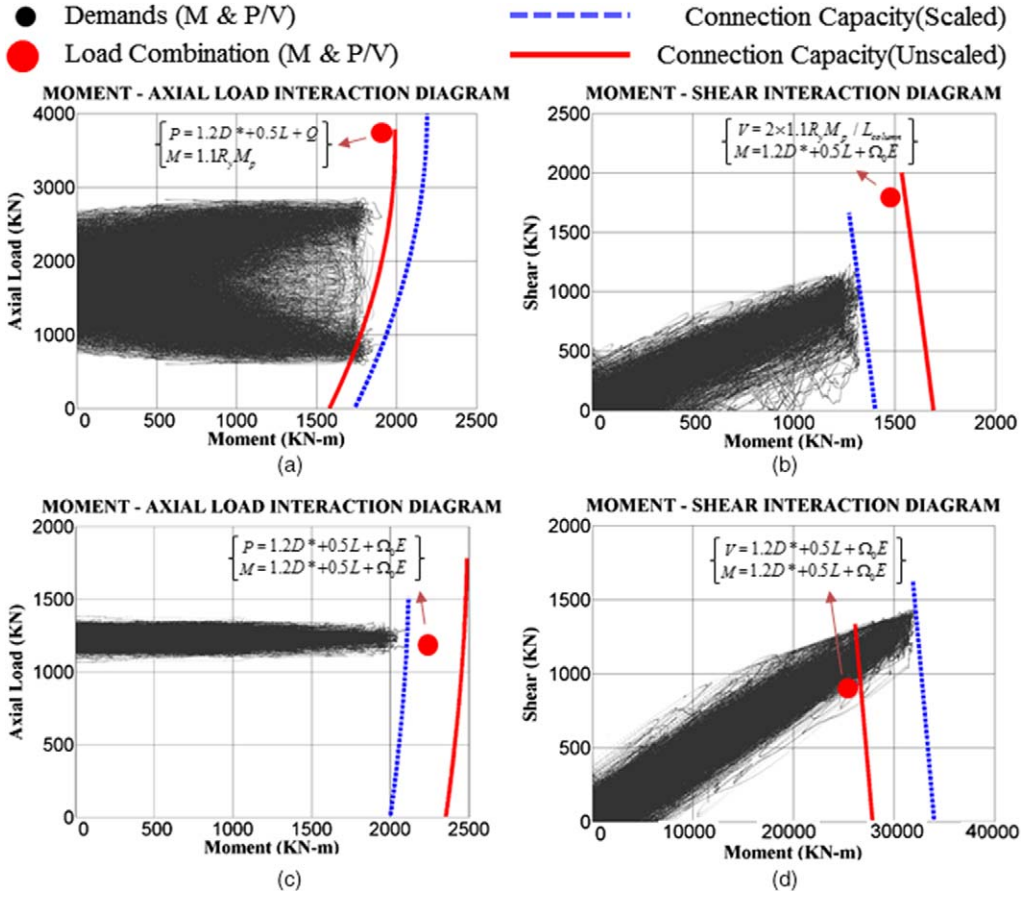

Figure 5. Demands and interaction curve for SMRF columns: (a) exterior column of 4-story SMRF, (b) exterior column of 12-story SMRF, (c) interior column of 4-story SMRF, and (d) interior column of 8-story SMRF.

3. A closer examination of the *P-M* interaction curve in Figure 5a indicates that the moment capacity increases with respect to axial compression near the horizontal axis. This may be attributed to the compressive prestress because of the axial load, which delays uplift of the base plate and subsequent limit states on the tension side of the connection (i.e., yielding of the base plate bending downwards or anchor rod yielding). A consequence of this response is that the critical condition (i.e., the demand point closest to the capacity curve) occurs at a low value of axial compression, rather than at its peak—as the moment capacity is lower. Following this, Table 2 also includes the normalized values of $P_{\min}$, denoting the minimum axial force for each configuration over all ground motions. Figure 5b is similar to Figure 5a, except it shows the response for embedded connections in the shear–moment (i.e., $V-M$) space determined as per methods outlined by Grilli and Kanvinde (2017). Unlike the $P-M$ interaction curve, presence of shear does not enhance the moment capacity.

In addition to Table 2, results are graphically presented in Figure 6a to 6h. Figure 6a and 6b correspond to the interior and exterior columns of the 2-story frame (i.e., the exposed base

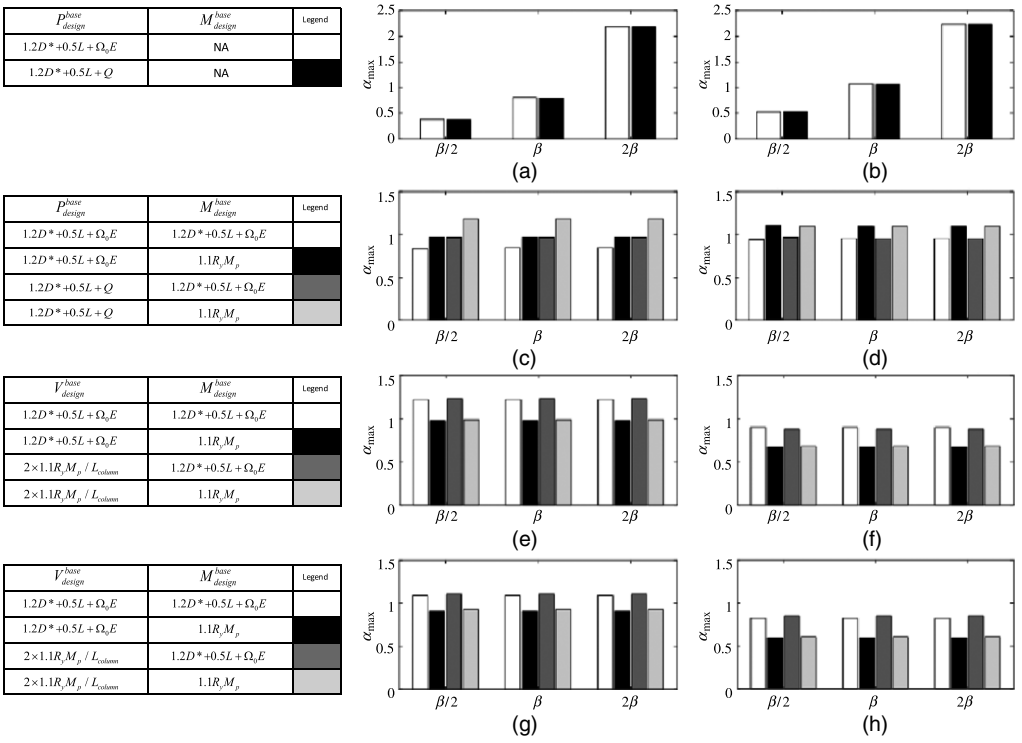

Figure 6. Variation of α_{max} with normalized base connection stiffness in SMRFs. (a), (b) interior, and exterior columns in 2-story SMRF; (c), (d) interior and exterior column in 4-story SMRF; (e), (f) interior and exterior column of 8-story SMRF; and (g), (h) interior and exterior column of 12-story SMRF.

plate connections). In both of these figures, the demand-capacity ratio $\alpha_{\max}$(maximum over all ground motions) is plotted against the normalized values of base stiffness (i.e., $\beta/2$, β, and 2β). The figures show two columns, each corresponding to one of the design configurations for the 2-story frame shown in Table 1. Recall that for all the exposed base connections, shear was not a design consideration, as all estimates of shear (including that based on yielding at both ends of the column) were well below the frictional capacity of the base. Figure 6c and 6d illustrate similar data for the 4-story frame. The difference in this case is that four columns are plotted to reflect the four design configurations for the bases connections of the 4-story frames. Figure 6e through 6h are similar to Figure 6c and 6d, except they reflect the design configuration and corresponding results for the 8- and 12-story frames, which feature the embedded base connections. The next section discusses the results presented in Table 2 and Figure 6a through 6h, along with implications for design of the base connections.

RESULTS AND IMPLICATIONS FOR DESIGN

Two-Story Frame (bases designed only for axial load as exposed base plate connections):

- Referring to Table 1, designs corresponding to both load combinations result in an identical connection configuration. As a consequence, the response for both is identical as well.
- For both the interior and exterior columns, the base moments are fairly low—in the range of 20%–25% of $1.1R_yM_p$. This may be attributed to the low stiffness of these connections, which are designed only for axial compression.
- The maximum axial compression $P_{\max}$ is greatest in the exterior columns, and is best estimated by P_{Ω_0}(which includes Dead, Live, and overstrength seismic load), such that $P_{\max}/P_{\Omega_0} = 0.84$ (the corresponding ratio for the capacity-based estimate $P_{\max}/P_Q = 0.72$. The axial compression is significantly lower for the interior columns (~40% of both the overstrength and capacity-based estimates), because of reduced overturning moment. Interestingly, the peak demand-capacity ratio $\alpha_{\max}$ for both cases is either close to critical (~0.8 for the interior columns) or slightly above critical (~1.07 for the exterior columns). A closer examination of the results (specifically, particle plots similar to Figure 5a) indicates that $\alpha_{\max}$ occurs not at the instant of maximum axial compression and moment, but rather when the axial compression is near its minimum value. This may be attributed to the shape of the $P-M$ interaction curve, which shows an increase in moment capacity with increasing axial compression by delaying uplift of the plate. This explains the somewhat high value of $\alpha_{\max}$ for the interior columns, which occurs despite the low levels of both peak axial force and moment. The main implication of this finding is that designing for minimum rather than maximum axial loads may be more suitable for design of exposed base plate connections, because the maximum axial loads (the increase flexural strength) may result in nonconservative designs.
- Motivated by the previous observation, Table 2 reports the minimum values of axial force $P_{\min}$; also reported are the estimates $P^-_{\Omega_0}$, and P^-_Q, which are similar to P_{Ω_0}, and P_Q except that overstrength or capacity axial forces are subtracted from the Dead and Live loads to include overturning induced tension. For the interior columns, the minimum forces are compressive, although both $P^-_{\Omega_0}$, and P^-_Q predict significant tension. For the exterior columns, the minimum forces are zero, whereas both

$P^{-}_{\Omega_0}$, and P^{-}_{Q}, again, predict significant tension. Based on the preceding point, this suggests that either estimate of column force $P^{-}_{\Omega_0}$, or P^{-}_{Q} will result in conservative design.

- Figure 6a and 6b show that for both the interior and exterior columns, the demand-capacity ratio $\alpha_{\max}$ increases strongly with base stiffness. Consequently, the appropriate design moment for these connections should account for the uncertainty in characterizing the base stiffness.
- Exposed base connections in moment frames are not usually shear-critical (Grilli and Kanvinde 2013). Nevertheless, the simulations (results for shear not shown in Table 2) indicate that the overstrength underestimates the peak shear ($V_{\max}/V_{\Omega_0} = 1.35$), whereas the shear calculated from capacity consideration significantly overestimates it ($V_{\max}/V_{M_p} = 0.47$).

Four-Story Frame (bases designed for axial load and moment, as exposed base plate connections):

- The peak moments in the 4-story frames (both design configurations) are approximately equal to $1.1R_yM_p$, indicating significant yielding and strain hardening. This may be attributed to their higher rotational stiffness, which is a result of their design for significant base moments (unlike the 2-story bases, which are designed only for axial force).
- All design configurations show response that is qualitatively similar to that observed for the 2-story frame (i.e., the critical condition occurs at an instant of low axial force and high moment). For the interior columns, all design combinations (except the one that utilizes P_Q and $1.1R_yM_p$) result in safe design (i.e., $\alpha_{\max} \leq 1$). For the exterior columns, the two combinations that utilize $[P_Q,\ M_{\Omega_0}]$, and $[P_{\Omega_0},\ M_{\Omega_0}]$ result in safe design, whereas those that use the $M^{base}_{design} = 1.1R_yM_p$ do not, presumably because for all exterior columns, $M_{\Omega_0} > 1.1R_yM_p$.
- Motivated by the previous points, Table 2 also includes $P_{\min}$ values along with counterpart estimates $P^{-}_{\Omega_0}$ and P^{-}_{Q}. The interior columns do not go into tension in any of the cases, and the estimates $P^{-}_{\Omega_0}$ are quite accurate, whereas the estimates P^{-}_{Q} predict significant tension in the column; this is conservative. The exterior columns too do not go into tension in any of the design cases. However, in each case the $P^{-}_{\Omega_0}$ and P^{-}_{Q} predict tension, which is conservative.
- Unlike the 2-story frame, the $\alpha_{\max}$ for all design cases of the 4-story base connections is quite insensitive to the base stiffness. This is because (as discussed previously) for all design combinations, the column base is fully yielded and plastified subjecting the base connection to $1.1R_yM_p$. Variations in stiffness change building deformations, but not the peak force and the $\alpha_{\max}$. In the 2-story frames, the column base moments are well below yield, and hence sensitive to base stiffness.
- The indicated overstrength underestimates the peak shear ($V_{\max}/V_{\Omega_0} = 1.24-1.34$), whereas the shear calculated from capacity considerations ($V_{\max}/V_{M_p} = 0.81-0.92$) is significantly more accurate.

Based on the previous observations, the following considerations are important for the design exposed base plate connections in low- to mid-rise moment frames:

1. Because of the beneficial effect of axial compression in exposed base plates, designing for peak moments and peak compression may not be conservative. The appropriate load combination includes the peak moment and the minimum anticipated axial load. The results indicate that use of either $P^{-}_{\Omega_0}$ and P^{-}_{Q} will result in conservative design, perhaps overly so.
2. For the 2-story frame (or more generally frames where the bases are designed as pinned), the true base moment is highly sensitive to base stiffness; this may result in yielding/fracture of the anchors. Even if the base is not expected to carry moment, this type of failure may be undesirable—for example, because it may reduce shear capacity of the connection. To mitigate this, it is important to design the base connection for some level of moment; using $M^{base}_{design} = 1.1R_yM_p$ is likely highly conservative. A more appropriate estimate of base moment may be obtained by simulating the structure (even in a linear elastic sense) with an estimated value of base stiffness. Kanvinde et al. (2012) provide a model to estimate base stiffness for exposed base plate connections.

Eight- and twelve-story frames (designed for moment and shear combinations, as embedded base connections). An analysis of results from the 8- and 12-story frames reveals similar insights. Consequently, they are discussed concurrently. The main observations are:

- For the interior column bases (all configurations), the peak moment demands $M_{\max}$ are very close to $1.1R_yM_p$ ($M_{\max}/1.1R_yM_p$ in the range of 0.97 to 0.99), and significantly greater than M_{Ω_0}, implying that the former estimate is accurate, possibly because the column bases undergo significant yielding. Additionally, for the interior columns, the only load combinations that result in safe design are those that include $M^{base}_{design} = 1.1R_yM_p$. For each of these cases, the peak demand-capacity ratio $\alpha_{\max}$ is very close to the corresponding $M_{\max}/1.1R_yM_p$. This indicates the flexural failure dominates failure, which is unsurprising because the interaction between the shear and moment is weak in the range of shear forces experienced by the base. Figure 5b shows this schematically; the weak interaction observed in this figure is representative of all connections examined in this study. Of the two combinations that use $M^{base}_{design} = 1.1R_yM_p$, the combination that uses $V^{base}_{design} = V_{M_p}$ is possibly more suitable for design, as it results in relatively accurate estimates of shear force across all interior column connections in these two frames ($V_{\max}/V_{M_p}$ in the range of 0.94 to 1.02, versus $V_{\max}/V_{\Omega_0}$ in the range of 1.40 to 1.55). However, because of the weak interaction between shear and moment, the effect of shear estimation on design is likely to be fairly modest.
- Even in the cases that do not result in acceptable design for the interior column bases (i.e., those corresponding to $M^{base}_{design} = M_{\Omega_0}$), the peak demand-capacity ratio $\alpha_{\max}$ is very close to the ratio $M_{\max}/M_{\Omega_0}$, providing further evidence that failure is moment-controlled.
- For the exterior column bases (all configurations), the peak moment demands $M_{\max}$ are better represented by M_{Ω_0} ($M_{\max}/M_{\Omega_0}$ in the range of 0.86 to 0.91) than by $1.1R_yM_p$($M_{\max}/1.1R_yM_p$ is in the range of 0.64 to 0.65). As the peak moments are well below $1.1R_yM_p$, the configurations that use $M^{base}_{design} = 1.1R_yM_p$ as a design

basis result in conservative designs ($\alpha_{\max}$ in the range of 0.61–0.68). On the other hand, the configurations that use $M_{design}^{base} = M_{\Omega_0}$ result in $\alpha_{\max}$ in the range of 0.82–0.90, indicating safe and less conservative design.

- For the exterior column bases, neither estimate of shear (i.e., V_{Ω_0} or V_{M_p}) is particularly accurate in characterizing peak shear demands ($V_{\max}/V_{\Omega_0}$ is in the range of 1.19–1.63, whereas $V_{\max}/V_{M_p}$ is in the range of 0.61–0.85). As for the interior column bases, the effect of shear on design is likely to be modest. Nevertheless, using $V_{design}^{base} = V_{M_p}$ is possibly the conservative choice.
- In all cases for the 8- and 12-story frames, the effect of base stiffness on $\alpha_{\max}$ is negligible.

In summary, for mid- to high-rise frames where column base connections are likely to be of the embedded type, the following design considerations are important:

1. Response is likely to be controlled by moment rather than shear; consequently, accurate characterization of moment is critical.
2. For the frames considered in this study, it appears that moment demands are well characterized by $1.1R_yM_p$ for interior column bases and by M_{Ω_0} for the exterior columns. Correspondingly, the design configurations that use these estimates result in successful (i.e., safe and economical) designs for both interior and exterior columns.
3. Although the effect of shear estimation on design is likely to be modest, using $V_{design}^{base} = V_{M_p}$ appears to be a reasonable and conservative approach.

SUMMARY AND CONCLUSIONS

Column base connections are critical components in steel moment frames subject to seismic loads, transferring axial forces, moments, and shears into the foundation. Previous research on these connections has focused on characterizing the response of the connections themselves, rather than the demands in these connections. Consequently, current design criteria for these connections are informed by conservatism and intuitive expectation of structural response, potentially resulting in uneconomical or unsafe design. In response, this study presents a series of nonlinear time history simulations on 2-, 4-, 8-, and 12-story steel moment-resisting frames, designed as per current U.S. practice. The base connections are also designed to reflect current practice; specifically, the 2- and 4-story frames feature exposed base plate type connections, whereas the 8- and 12-story frames feature embedded connections. Each connection is designed for multiple design load combinations with axial forces, moments, and shears calculated either from overstrength or capacity considerations. The simulations employ state of the art methodologies to model material and geometric nonlinear response, and are subjected to a suite of 40 ground motions scale to represent design-level (i.e., 10% probability of exceedance in 50 years) seismic hazard. The main findings and design implications from the simulation results may be briefly synthesized as follows:

- When exposed base plate connections are specified, failure is likely to be controlled by the minimum axial compression (or maximum tension) accompanied by high moment. This is because of the beneficial effects of axial compression that delay uplift of the base plate and associated limit states of base plate or anchor rod yielding. The axial load corresponding to this condition may be conservatively

estimated by subtracting either the overstrength or capacity-based axial overturning force from the dead and live load effects.

- Even if designed as pinned (e.g., in low-rise frames), exposed base plate connections are susceptible to flexural yielding and failure, which may compromise connection integrity. Moreover, the demands on these connections are highly sensitive to base stiffness; it is prudent to estimate design loads through linear elastic simulations that represent this base stiffness.
- When embedded base connections are specified, the response is largely controlled by moment. The results indicate that overstrength-based estimates of moments are accurate for exterior column bases, whereas capacity-based estimates are accurate for interior ones; this trend may not be general and it is advisable to use capacity-based estimates in all cases.

This study has several limitations, which must be considered in its interpretation and generalization. The range of variables interrogated, such as the building plans, heights, and designs (other design solutions are possible for the same conditions, especially if a corner column is shared between two orthogonal lateral load resisting systems) limit the generality of the findings. Similarly, biases because of ground motion effects, including the effects of vertical component of ground motions, cannot be entirely eliminated. For the quantity (i.e., the base stiffness) that is expected to have the greatest influence on results, a sensitivity study is conducted and reported in this study. However, the response may be sensitive to other modeling assumptions as well; these include the use of concentrated plasticity (versus distributed plasticity), the selection of hysteretic model functional forms and parameters, and lack of consideration of soil-structure interaction (SSI) effects. Finally, the simulations are all based on a design-level hazard and the intent of design standards that base connections must remain elastic at this intensity of shaking. As a result, the study does not address response (e.g., base connection yielding because of overloads) that may occur at higher intensities of shaking.

ACKNOWLEDGMENTS

The authors would like to thank The National Secretariat of Higher Education, Science, Technology, and Innovation of Ecuador (SENESCYT) whose graduate fellowship provided support for the lead author.

REFERENCES

American Concrete Institute (ACI), 2014. *Building Code Requirements for Structural Concrete (ACI 318-14)*, Farmington Hills, MI.

American Institute of Steel Construction (AISC), 2006. *Seismic Design Manual*, Chicago, IL.

American National Standards Institute/American Institute of Steel Construction (ANSI/AISC), 2010. *Seismic provisions for structural steel buildings, ANSI/AISC 341-10*, Chicago, IL.

American Institute of Steel Construction (AISC), 2011. *Steel Construction Manual, 14th Edition*, Chicago, IL.

American National Standards Institute/American Institute of Steel Construction (ANSI/AISC), 2016. *Seismic provisions for structural steel buildings, ANSI/AISC 341-16*, Chicago, IL.

American National Standards Institute/American Institute of Steel Construction (ANSI/AISC), 2016. *Prequalified connections for special and intermediate steel moment frames for seismic applications, ANSI/AISC 358-16*, Chicago, IL.

American Society of Civil Engineers/Structural Engineering Institute (ASCE/SEI), 2006. *Minimum Design Loads for Buildings and Other Structures, ASCE/SEI 7-05*, Reston, VA.

Applied Technology Council (ATC), 2010. *ATC 72-1, Modeling and Acceptance Criteria for Seismic Design and Analysis of Tall Buildings*, Redwood City, CA.

Astaneh, A., Bergsma, G., and Shen, J. H., 1992. Behavior and design of base plates for gravity, wind and seismic loads, in *Proceedings of the National Steel Construction Conference*, June 1992, Las Vegas, NV.

Barnwell, N., 2015. Experimental Testing of Shallow Embedded Connections Between Steel Columns and Concrete Footings, Master's Thesis, Brigham Young University.

Fisher, J. M., and Kloiber, L. A., 2006. Base plate and anchor rod design, 2nd ed., in *Steel Design Guide Series No. 1*, American Institute of Steel Construction, Inc., Chicago, IL.

Gomez, I. R., Kanvinde, A. M., and Deierlein, G. G., 2010. *Exposed column base connections subjected to axial compression and flexure*, Report Submitted to the American Institute of Steel Construction (AISC).

Grilli, D. A., and Kanvinde, A. M., 2013. Special Moment Frame Base Connection: Design Example 8, *2012 IBC SEAOC Structural/Seismic Design Manual*, Volume 4, Examples for Steel-Frame Buildings, 255–280.

Grilli, D. A., and Kanvinde, A. M., 2017. Embedded column base connections subjected to seismic loads: strength model, *Journal of Constructional Steel Research* **129**, 240–249.

Gupta, A., and Krawinkler, H., 1999. Prediction of seismic demands for SMRFs with ductile connections and elements, *SAC Joint Venture, 2002*.

Ibarra, L. F., Medina, R. A., and Krawinkler, H., 2005. Hysteretic models that incorporate strength and stiffness degradation, *Earthquake Engineering and Structural Dynamics* **34**, 1489–1511.

Kanvinde, A. M., Grilli, D. A., and Zareian, F., 2012. Rotational stiffness of exposed column base connections: Experiments and analytical models, *Journal of Structural Engineering* **138**(5), 549–560.

Kanvinde, A. M., Jordan, S. J., and Cooke, R. J., 2013. Exposed column base plate connections in moment frames—simulations and behavioral insights, *Journal of Constructional Steel Research* **84**, 82–93.

Lignos, D. G., and Krawinkler, H., 2011. Deterioration modeling of steel components in support of collapse prediction of steel moment frames under earthquake loading, *ASCE Journal of Structural Engineering* **137**, 1291–1302.

McKenna, F., Fenves, G. L., and Scott, M. H., 2000. *Open System for Earthquake Engineering Simulation*, University of California, Berkeley, Berkeley, CA.

Medina, R. A., and Krawinkler, H. 2003. *Seismic demands for nondeteriorating frame structures and their dependence on ground motions, Report No. 144*, John A. Blume Earthquake Engineering Center, Department of Civil Engineering, Stanford University, Stanford, CA.

National Earthquake Hazards Reduction Program (NEHRP), 2010. *Evaluation of the FEMA P-695 Methodology for Quantification of Building Seismic Performance Factors, NIST GCR 10-917-8*, NEHRP Consultants Joint Venture.

Richards, P. W., 2009. Seismic column demands in ductile braced frames, *Journal of Structural Engineering* **135**(1), 33–41.

Stamatopoulos, G. N., and Ermopoulos, J. Ch., 2011. Experimental and analytical investigation of steel column bases, *Journal of Constructional Steel Research* **67**, 1341–1357.

Structural Engineers Association of Central California (SEAOC), 2015. *2015 IBC SEAOC Structural/Seismic Design Manual Volume 1: Code Application Examples*, Structural Engineers of California.

Torres-Rodas, P., Zareian, F., and Kanvinde, A., 2017. Rotational stiffness of deeply embedded column–base connections, *ASCE Journal of Structural Engineering* **142**(8), 04017064.

Trautner, C., Hutchinson, T., Grosser, P., and Silva, J., 2016. Effects of detailing on the cyclic behavior of steel baseplate connections designed to promote anchor yielding, *ASCE Journal of Structural Engineering* **142**(2), 04015117.

Zareian, F., and Kanvinde, A. M., 2013. Effect of column base flexibility on the seismic safety of steel moment resisting frames, *Earthquake Spectra* **29**(4), 1–23.

Zareian, F., and Krawinkler, H., 2009. *Simplified performance-based earthquake engineering, Report No. 169*, John A. Blume Earthquake Engineering Center, Department of Civil Engineering, Stanford University, Stanford, CA.

(Received 23 June 2017; accepted 25 February 2018)